Analytical fittings for the global potential energy surface of the ground state of methylene

Jen-Shiang K. Yu, Sue-ying Chen, and Chin-Hui Yu[a)]
Department of Chemistry, National Tsing Hua University, Hsinchu 300, Taiwan

(Received 11 July 2002; accepted 1 October 2002)

The global potential energy surface (PES) corresponding to the dissociation reaction of the ground state of methylene (CH_2) is studied with the coupled-cluster method with single, double and perturbative triplet excitations, CCSD(T), in conjunction with the correlation-consistent cc-pVTZ basis set, and fitted by three analytical potential functions in terms of the Simons–Parr–Finlan (SPF) polynomial, Jensen function and the Sorbie–Murrell (SM) function. *Ab initio* single-point calculations over a distributed range of grids are performed first, and totally 12 085 converged points are fed into these functions. The fitting of each analytical PES function is done with an unconstrained minimization of the difference between the evaluations of the analytical function and the *ab initio* results, solved by a modified Levenberg–Marquardt algorithm with a finite-difference Jacobian in the IMSL package. The SPF polynomial is found to have the best global description, while the SM function behaves superior in the dissociation region forming three atoms. The spline function is potentially feasible to interpolate the computationally divergent points in the *ab initio* calculations. © *2003 American Institute of Physics.* [DOI: 10.1063/1.1523906]

I. INTRODUCTION

Potential energy surfaces (PES) are essential in chemical process studies. The actual reaction path of molecules[1] in terms of encounter depends on their total energies, which are the sum of the kinetic and the potential energies. However, PES alone provides primary insights of possible pathways, which correspond to the minimal potential energy that are the most important. Experimentally, the task considering how the molecules move through their PES when they as well possess kinetic energy can be explored by molecular beam studies. Dynamical calculations,[2] namely the calculations for cross sections, rate constants, transition probabilities, or dynamical attributes such as threshold energies, require analytical PES functions. Chemical dynamics produces results comparable to experimental measurements while highly accurate potential energy functions as well as extra details from the theoretical outputs are available. For example, theoretical investigations may either generate information about the dependence of cross sections on the initial vibrational states if only the initial translational energy is experimentally varied, or yield rotational distributions of products provided the experimental product-state resolution is merely sufficient to distinguish vibrational structure. In other cases, theoretical rate calculation for systems that no experiments have been performed is possible. Moreover, dynamic theories can provide opacity functions, which are transition probabilities as a function of the impact parameter and are absolutely unattainable by experiments. The disadvantages over potential energy surfaces are that for many systems the PES lacks of either chemical accuracy or demonstrated reliability, and on the other hand additional errors are possibly introduced by the dynamical calculations. Thus further improvements are required in this field of potential energy surfaces combined with dynamics calculations.

Methylene radical,[3] CH_2, is the simplest polyatomic molecule of which the ground state is a triplet state and having a very low-lying singlet excited state. The electronic characteristics make methylene rather unusual chemical and physical properties. Depending on its multiplicity, the radical adds differently to olefins.[4] Methylene is also the simplest carbene, which is an important intermediate in various organic reactions. In addition, methylene is a product of the photolysis reaction of diazomathane (CH_2N_2),[5] or ketene (CH_2CO).[6] Carbenes[7] share the common isoelectronic property with the two generally accessible electronic singlet and triplet states. The singlet electronic state appears as an electrophile and/or a nucleophile whereas the triplet electronic state possesses radical properties. Therefore, carbenes are related to ''the reactive intermediate'' and are simultaneously classically stable species. In the interstellar space,[8,9] although not firmly identified, CH_2 is the direct precursor of the widely observed CH radical and other carbon-bearing molecules. Nevertheless, CH_2 is in addition considered as an important link in the Lyman α-band photodissociation sequence of cometary methane. The CH_4 photodissociates into CH_2, and further dissociates to form $CH+H$ or $C+H_2$ photochemically. In the aforementioned sequence, CH is the only observable species. Studies on CH and CH_4 have been done in detail and the largest uncertainty lies on the photodissociation rate of CH_2 as well as the branching ratio to form CH or C.

Many theoretical studies have been done for the PES of methylene.[10–19] The most accurate result to date has been done by Comeau *et al.*[16] using the multireference configuration-interaction (MRCI) method with a large basis

[a)]Author to whom correspondence should be addressed. Electronic mail: chyu@oxygen.chem.nthu.edu.tw; Fax: +886-3-5721534.

set of $[5s4p3d2f1g/3s2p1d]$. Totally 45 points were reported, focusing on the region close to the minimum. Those points were then fitted by Morse-oscillator rigid bender internal dynamics (MORBID) procedure[20,21] to get the rotational-vibrational energy levels. The semiempirical potential by Jensen and Bunker[15] is probably very accurate description in the region near the minimum. They adjusted nine out of the 24 parameters in the same *ab initio* potential used by Comeau *et al.* to improve the agreement between the predicted and the observed rotational-vibrational energy levels. As for the global potential, Knowles, Handy, and Carter[12] reported complete active-space self-consistent field (CASSCF) calculations employing the $[5s3p2d/2s1p]$ basis set on the two lowest $3A''$ states. These data points have been scaled to match the experimental dissociation energy prior to fit a potential function, which is in the form of a diagonalized 2 by 2 matrix and describes well around the conical intersections between the two lowest triplet surfaces that occur at linear geometries.

Recently Harding, Guadagnini, and Schatz[18] carried out calculations of about 6000 points on the ground state potential surface of methylene by MRCI/$(4s3p2d1f/3s2p1d)$ level of theory. Four stationary points were reported with $^3B_1$, $^3A_2$, $^3\Pi$, and $^3\Sigma^-$ symmetries, respectively. The resultant energies were fit to a many-body expansion and conical insertions between the $^3B_1$ and $^3A_2$ states for C_{2v} geometries and between the $^3\Pi$ and $^3\Sigma^-$ states for linear geometries are also included. No barrier is predicted for either CH+H addition or C+H_2 insertion reactions. The entrance channel of CH+H addition reaction is very broadly attractive and the long-range approaching force becomes repulsive only when geometries are close to linear. On the $^3A_2$ surface the repulsion increases at shorter distances and the energy is minimum at long range. Furthermore, no barrier exists and a loosely bound complex is formed for the C+H_2 addition. The C_{2v} conical insertion between $^3B_1$ and $^3A_2$ surfaces is predicted to be important in determing the topology of the surface in the neighborhood of C+H_2 insertion reaction path.

It is aimed for obtaining the global potential energy surface of the triplet ground state methylene in this study. According to the correlation diagram,[15] CH_2 dissociates via two possible channels: $C(^3P)+H_2(^1\Sigma_g^+)$ and $CH(^2\Pi)+H(^2S)$. The global potential energy surface functions are deduced by the following procedure. High level *ab initio* calculations at more than ten thousand of molecular geometries are carried out, followed by the fitting of the parameters of the analytical potential energy functions.

II. COMPUTATIONAL DETAILS

Many-body methods for electron correlation are used due to the size consistent requirement in considering the dissociation channels. Coupled-cluster method with single, double and perturbative triplet excitations, CCSD(T),[22] are used in conjunction with Dunning's correlation-consistent cc-pVTZ basis set. The CCSD(T) calculations are performed with the ACES II program.[23]

The most efficient strategy to proceed with electronic structure calculations on numerous points over the extension of a global potential energy surface is to scan the surface stepwise starting from the equilibrium geometry. The initial guess of the molecular orbitals (MOs) of one certain geometry is the converged molecular orbitals of the preceding point. For CH_2 molecule, the single-point calculations are done with separate groups of computations, in terms of the C_{2v} symmetry and those with C_s symmetry in order to take the advantage of molecular symmetry with proper initial MO guesses.

In order to cover the complete dissociation routes, grids over a large range of bond length and bond angle are used. The coordinates initially chosen to perform high level *ab initio* calculations are shown in Table I. It generates 28 101 points ($57\times29\times17$). Nevertheless, denser grids are aimed at the region near the equilibrium structure, while sparser grids are chosen for large bond lengths and small bond angles in order to save computational resources. Three empirically derived analytical potential energy functions, in terms of the Simons–Parr–Finlan (SPF) polynomial, Jensen function and the Sorbie–Murrell (SM) function, plus the bivariate spline function which is one of the most frequently employed all-numerical fitting among the numerical methods, are employed to fit to the results by *ab initio* calculations. The mathematical form and algorithms of each analytical function is described in detail in the Appendix.

The fitting of each analytical PES function is an unconstrained minimization of a continuous many-variable function. This nonlinear least-square problem can be solved by a modified Levenberg–Marquardt algorithm with a finite-difference Jacobian, implemented by the subroutines UNLSF/DUNLSF within the IMSL[24] package. The bivariate spline interpolation is done by the SURF/DSURF subroutine in the identical IMSL package.

III. RESULTS AND DISCUSSIONS

Table II contains the equilibrium properties of C, H, CH, H_2 in their ground states calculated by the same CCSD(T)/cc-pVTZ level used in CH_2 calculations. In Table II, the results by CCSD/TZ2P and CCSD(T)/cc-pVTZ together with those of literatures are listed. The computation by Comeau *et al.*[16] is regarded the historically most accurate *ab initio* calculation. Their optimized C–H bond distance was 1.071 Å, ∠HCH angle was 132.9° and energy was −39.087 452 hartree, and our calculated energy at CCSD(T)/cc-pVTZ is lower by 0.006 652 4 hartree. Experimentally,[14] the bond distance is 1.0748 ± 0.0004 Å, and the bond angle is $133.84°\pm0.05°$. The geometry at the level of CCSD/TZ2P is very close to the experimental values; however, due to its poor level of theory and small basis set, this match is regarded as a coincidence. For the vibrational spectrum of CH_2, only the fundamental bending frequency[2] has been measured[25] to be 963.10 cm^{-1}. The frequency of this mode is 1128 cm^{-1} according to CCSD/TZ2P. The fundamental frequencies of the two stretching modes, 1 and 3 are still not clear for their very weak intensity. The calculation done by Comeau *et al.* yielded these two modes at 3013 and 3235 cm^{-1}, while our study reports 3173 and 3395 cm^{-1} by

TABLE I. The combination of coordinate grids for the global PES calculation of CH_2 with CCSD(T)/cc-pVTZ method. The numbers in bold face are of the equilibrium structure.

$R_{CH}^{(1)}$ (Å)	$R_{CH}^{(1)}$ (Å) *cont.*	$R_{CH}^{(2)}$ (Å)	∠HCH (degrees)
1.023 519	1.666 469	1.018 227	24.126 806
1.028 810	1.732 616	1.028 810	44.126 806
1.036 748	1.798 763	10.44 686	64.126 806
1.044 686	1.864 910	1.055 269	84.126 806
1.049 977	1.931 057	1.065 853	94.126 806
1.055 269	1.997 204	**1.071 145**	104.126 806
1.060 561	2.063 351	1.097 603	114.126 806
1.065 853	2.129 499	1.113 479	124.126 806
1.071 145	2.195 646	1.124 062	129.126 806
1.081 728	2.261 793	1.150 521	**134.126 806**
1.092 312	2.327 940	1.176 980	139.126 806
1.097 603	2.394 087	1.203 439	144.126 806
1.102 895	2.460 234	1.335 733	149.126 806
1.108 187	2.526 381	1.468 027	154.126 806
1.113 479	2.658 676	1.600 322	159.126 806
1.118 770	2.790 970	1.732 616	164.126 806
1.124 062	2.989 411	1.864 910	174.126 806
1.137 292	3.187 853	1.997 204	
1.150 521	3.452 441	2.129 499	
1.163 751	3.717 030	2.261 793	
1.176 980	4.444 648	2.394 087	
1.190 209	5.172 266	2.526 381	
1.203 439	6.495 209	2.790 970	
1.269 586	7.818 151	3.187 853	
1.335 733	9.141 094	3.717 030	
1.401 880	10.464 036	5.172 266	
1.468 027	11.786 979	7.818 151	
1.534 174	13.109 921	10.464 036	
1.600 322		13.109 921	

CCSD/TZ2P. The algorithm to calculate vibrational frequencies with CCSD(T) method is not yet available in ACES II, and therefore the values are not listed.

The ground state of CH_2 correlates with the ground states of CH+H and $C+H_2$. From *ab initio* results at the level of CCSD(T)/cc-pVTZ, the sums of energy of separate atoms are −38.791 636 43 hartree for C+H+H, −38.923 471 19 hartree for CH+H and −38.964 470 52 hartree for $C+H_2$, respectively. Figure 1 shows the relative energy levels. Results of *ab initio* calculation featuring unreasonable energies are omitted according to the following examination. Points with energies higher than −38.791 636 43 hartree, which is the sum of energies of three separate atoms, are deleted. The number of data points is reduced to 12 085 out of the original computationally converged 12 448 points by the filtration.

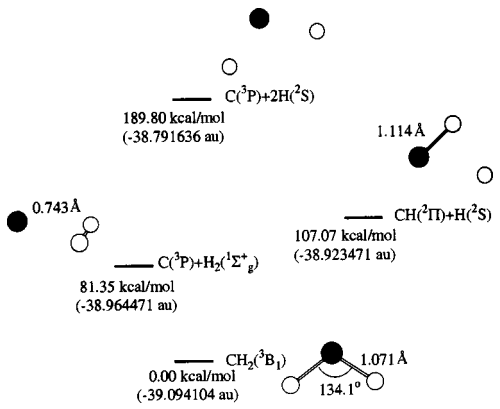

FIG. 1. The relative energy levels of the dissociation of CH_2 at CCSD(T)/cc-pVTZ level of theory.

In our initial test using the SPF polynomial, only terms up to quartic expansions were considered, however, the DUNLSF subroutine of IMSL package failed to minimize due to insufficient number of parameters. Thus the terms of the fifth order are taken into consideration. The SM function has the most complex form comparing with the other two for the reason that several Taylor series transformations are necessary to generate the coefficients in the polynomial $P(s_1,s_2,s_3)$. The zero of energy of the SM function is defined as the ground state of the three separate atoms (C+H+H). Although there are only five explicit parameters (c_0, A, γ_1, γ_2, γ_3) in the SM function, those force constants in Eq. (14) must be also included as parameters for optimization in order to yield satisfactory results. Thus the number of parameters to be optimized therefore increases from 5 to 21.

Table III reports the fitted values of parameters determined in each analytical potential function. Both of the SPF polynomial and Jensen functions behave satisfying in regenerating the exact equilibrium geometry and energy of the *ab initio* data. Since the zero of the fitted SM function is defined as the three separate atoms, its failure to reproduce the optimized structure of CCSD(T)/cc-pVTZ is within expectation. The relative energy evaluated by the SM function at the equilibrium geometry is −2.313 kcal/mol.

TABLE II. The optimized structures, energies, and harmonic frequencies of all the species involved in the CH_2 dissociation reaction at various levels of theories.

	CCSD/TZ2P	CCSD(T)/cc-pVTZ	MRCI/[5*s*4*p*3*d*2*f*1*g*/3*s*2*p*1*d*][a]	Experimental value
R_{CH}(Å)	1.075	1.071	1.078	1.0748±0.0004[b]
∠HCH(°)	133.3	134.1	132.9	133.84±0.05[b]
Energy (a.u.)	−39.082 891 0	−39.094 104 4	−39.087 452	-
ν_1 (cm^{-1})	1128	1085	969[a]	963.10[c]
ν_2 (cm^{-1})	3173	3167	3013[a]	-
ν_3 (cm^{-1})	3395	3369	3235[a]	-
ZPE (kcal/mol)	11.00	10.90	10.61	-

[a]Reference 16. The frequencies are fitted by the MORBID procedure.
[b]Reference 25.
[c]Reference 25.

TABLE III. The fitted parameters of the SPF polynomial, Jensen function and the SM function.

The SPF polynomial		Jensen function		The SM function	
L_{11}	373.262 11	a_1	0.707 31	γ_1	0.916 55
L_{22}	384.810 71	a_3	0.707 31	γ_2	0.916 55
L_{33}	149.188 61	$f_0^{(2)}$	32.989 51	γ_3	−0.556 71
L_{12}	184.761 82	$f_0^{(3)}$	48.231 92	A	106.951 87
L_{13}	12.877 56	$f_0^{(4)}$	141.214 87	c_0	−0.057 34
L_{23}	16.608 11	$f_0^{(5)}$	−729.714 44	c_1	0.458 27
L_{111}	1026.623 52	$f_0^{(6)}$	1088.702 26	c_2	0.458 27
L_{222}	1021.463 50	$f_0^{(7)}$	−679.807 33	c_3	−0.278 35
L_{333}	97.635 69	$f_0^{(8)}$	152.717 31	c_{11}	1.425 68
L_{112}	−471.266 28	$f_1^{(1)}$	−46.504 29	c_{22}	1.425 68
L_{113}	195.985 74	$f_1^{(2)}$	82.358 71	c_{33}	4.766 93
L_{122}	−510.491 50	$f_1^{(3)}$	−84.864 37	c_{12}	1.175 96
L_{133}	−116.314 61	$f_1^{(4)}$	−2.723 91	c_{13}	−3.090 76
L_{223}	206.433 90	$f_3^{(1)}$	−46.504 29	c_{23}	−3.090 76
L_{233}	−126.820 30	$f_3^{(2)}$	82.358 71	c_{111}	1.726 68
L_{123}	−73.404 38	$f_3^{(3)}$	−84.864 37	c_{222}	1.726 68
L_{1111}	−2821.907 73	$f_3^{(4)}$	−2.723 91	c_{333}	−1.441 95
L_{2222}	−2885.250 47	$f_{11}^{(0)}$	874.375 86	c_{112}	0.822 40
L_{3333}	20.113 33	$f_{11}^{(1)}$	−57.754 38	c_{113}	0.812 19
L_{1112}	−87.387 86	$f_{11}^{(2)}$	−236.382 37	c_{122}	0.822 40
L_{1113}	−409.868 80	$f_{11}^{(3)}$	97.281 30	c_{133}	−0.625 81
L_{1122}	1070.938 65	$f_{33}^{(0)}$	874.375 86	c_{223}	0.812 19
L_{1133}	−3.093 60	$f_{33}^{(1)}$	−54.754 38	c_{233}	−0.625 81
L_{1123}	−78.966 79	$f_{33}^{(2)}$	−236.382 37	c_{123}	1.457 37
L_{1222}	34.623 05	$f_{33}^{(3)}$	97.281 30	f_{11}	1865.432 53
L_{1333}	−62.883 38	$f_{13}^{(0)}$	−92.594 47	f_{22}	1865.432 53
L_{1223}	−39.909 65	$f_{13}^{(1)}$	24.004 56	$f_{\alpha\alpha}$	317.336 06
L_{1233}	20.172 46	$f_{13}^{(2)}$	70.598 44	f_{12}	1064.107 08
L_{2223}	−486.281 43	$f_{13}^{(3)}$	10.176 22	$f_{1\alpha}$	567.800 66
L_{2233}	−12.136 07	$f_{111}^{(0)}$	−1305.358 98	$f_{2\alpha}$	567.800 66
L_{2333}	−71.547 02	$f_{111}^{(1)}$	313.436 78	f_{111}	−6987.165 09
L_{11111}	1546.832 00	$f_{111}^{(2)}$	91.816 97	f_{222}	−6987.165 09
L_{22222}	1606.063 56	$f_{333}^{(0)}$	−1305.358 98	$f_{\alpha\alpha\alpha}$	−1475.499 87
L_{33333}	1.202 20	$f_{333}^{(1)}$	313.436 78	f_{112}	−4514.566 36
L_{11112}	335.165 05	$f_{333}^{(2)}$	91.816 97	$f_{11\alpha}$	−1486.683 12
L_{11113}	212.756 02	$f_{113}^{(0)}$	55 201 200.582 55	f_{122}	−4514.566 36
L_{11122}	−406.601 85	$f_{113}^{(1)}$	−4 825 301.068 28	$f_{1\alpha\alpha}$	−1283.709 23
L_{11133}	8.597 49	$f_{113}^{(2)}$	−27 649 651.991 15	$f_{12\alpha}$	−1632.000 74
L_{11123}	43.310 81	$f_{133}^{(0)}$	−55 201 193.942 42	$f_{22\alpha}$	−1486.683 12
L_{11222}	−410.592 25	$f_{133}^{(1)}$	4 825 354.852 28	$f_{2\alpha\alpha}$	−1283.709 23
L_{11333}	0.956 83	$f_{133}^{(2)}$	27 649 625.242 30		
L_{11223}	103.271 45	$f_{1111}^{(0)}$	546.375 07		
L_{11233}	0.103 60	$f_{1111}^{(1)}$	−210.262 70		
L_{12222}	254.168 64	$f_{3333}^{(0)}$	546.375 07		
L_{13333}	−8.485 25	$f_{3333}^{(1)}$	−210.262 70		
L_{12223}	45.391 25	$f_{1113}^{(0)}$	33.864 79		
L_{12233}	10.242 89	$f_{1113}^{(1)}$	26.719 71		
L_{12333}	5.721 53	$f_{1133}^{(0)}$	−14.021 65		
L_{22223}	261.663 81	$f_{1133}^{(1)}$	−126.251 78		
L_{22233}	7.578 51	$f_{1333}^{(0)}$	27.735 02		
L_{22333}	−0.214 97	$f_{1333}^{(1)}$	11.083 25		
L_{23333}	−9.828 71				

A summary of fitting error is given in Table IV: The calculated points are sorted by the energy relative to the CH_2 minimum and grouped into ranges with the interval of 10 kcal/mol. Two statistical factors are used to illustrate the fitting error: the standard deviation (STDEV) and the root mean square (rms). Near the equilibrium geometry where the energy range is between 0 and 30 kcal/mol, the SPF polynomial and the Jensen function reproduce well with an rms error of less than 1.773 kcal/mol. Within the range of 40–60 kcal/mol above the ground state of CH_2, the fitting results of these two functions are also superior with STDEV less than 0.963 kcal/mol and rms error less than 1.641 kcal/mol. At the energy range of 160–170 kcal/mol above the minimum, the SPF polynomial and Jensen function behave the worst. The SM function acts relatively inferior at the energy of 170–180 kcal/mol, but has the best description around the range of 100–120 kcal/mol. For the global PES, the SPF polynomial has the smallest STDEV as well as the smallest rms error. In Table V, the SPF polynomial, Jensen function, and the SM function yield 86%, 62%, and 66% respectively, out of the

TABLE IV. The fitting errors of the three analytical functions. The unit of the energies is in kcal/mol. The zero of the PES is shifted to $CH_2(^3B_1)$.

Energy range	No. of points	Energy deviation ($V_{fit}-V_{ab\ initio}$) SPF min	SPF max	Jensen min	Jensen max	SM min	SM max	Standard deviation of ($V_{fit}-V_{ab\ initio}$) SPF	Jensen	SM	Root mean square error of ($V_{fit}-V_{ab\ initio}$) SPF	Jensen	SM
0–10	1622	−1.606	5.985	−1.049	1.207	−5.191	2.607	1.201	0.399	1.575	1.248	0.400	1.792
10–20	487	−1.741	2.842	−0.284	2.014	−0.539	4.390	0.998	0.621	1.406	1.219	1.147	2.536
20–30	286	−1.478	4.984	−0.318	3.146	−0.839	6.477	1.366	0.823	1.941	1.773	1.685	3.510
30–40	343	−1.223	5.767	−0.390	3.130	−1.751	6.482	1.537	0.904	2.312	2.425	2.087	4.068
40–50	258	−0.831	3.481	−0.479	2.914	−2.139	5.944	0.936	0.681	2.087	1.560	1.641	2.741
50–60	216	−0.597	4.190	−0.752	2.912	−2.801	4.489	0.963	0.739	1.755	1.467	1.590	2.307
60–70	326	−1.185	10.442	−0.936	5.801	−3.039	3.502	2.764	1.464	1.467	3.524	2.142	1.527
70–80	355	−3.524	4.560	−2.681	6.647	−3.392	10.432	1.332	1.445	2.093	1.359	1.617	2.097
80–90	582	−16.115	25.509	−20.881	31.865	−25.839	10.805	3.728	5.199	3.863	3.733	5.431	3.895
90–100	817	−17.744	29.651	−24.122	34.812	−32.520	10.178	5.630	7.387	7.787	5.810	7.437	8.396
100–110	2087	−16.773	33.662	−25.337	36.981	−34.952	17.117	4.901	4.870	4.796	5.628	5.765	4.899
110–120	886	−18.083	30.744	−27.224	32.873	−15.061	16.699	6.148	5.939	4.911	6.303	5.988	4.912
120–130	1463	−22.581	18.801	−26.265	25.044	−19.481	13.950	6.431	5.903	7.916	7.499	7.468	11.998
130–140	363	−23.499	29.850	−35.248	31.418	−22.149	14.858	8.339	9.344	7.945	8.559	9.479	7.941
140–150	223	−27.704	23.502	−42.491	25.911	−23.226	13.742	7.995	9.435	8.168	7.984	9.490	8.223
150–160	239	−33.556	29.712	−31.365	28.342	−24.086	30.404	7.987	8.803	7.475	8.159	8.932	7.563
160–170	196	−44.703	31.709	−34.411	31.738	−25.075	28.729	9.961	10.028	10.255	9.941	10.014	11.113
170–180	301	−39.021	19.759	−36.515	18.535	−24.744	16.643	7.358	8.167	10.474	7.959	8.574	11.325
180–190	1035	−27.441	12.487	−30.282	17.615	−36.848	5.948	6.154	6.372	8.461	6.519	6.780	11.143
0∼190	12 085	−44.703	33.662	−42.491	36.981	−30.404	30.404	5.535	5.846	6.894	5.536	5.846	7.130

total 12 085 points with an error within ±5% of energy deviation from the corresponding *ab initio* result. The SPF polynomial has the highest accuracy for reproducing *ab initio* values while the SM function is less accurate.

Figures 2 and 3 illustrate the energy curves of computed *ab initio* energies and corresponding fitted energies as functions of bond distances of C–H with constant ∠HCH angles of 39° and 134.1°. The PES curve drawn in Fig. 2 are those with one C–H bond being fixed at its equilibrium value of 1.071 Å as well as the ∠HCH angles being constrained at 134.1°. The energy curves distribute from 0 to 100 kcal/mol relative to the ground state CH_2 while the other C–H bond lies between 1 and 3 Å. All energy curves have similar shape: Curves move upward with minima located around the equilibrium bond length of 1.071 Å. In this region all three potential functions show this tendency; however, the SPF polynomial and Jensen function are more accurate. For very small bond length (<0.8 Å), the SPF polynomial expansion presents incorrect energetic tendency due to its polynomial nature without empirical terms [Fig. 2(a)]; Jensen function and the SM function have correct descriptions for their Morse-like shape. This disadvantage of the SPF polynomial still exists even the constraint of the first C–H bond increases to 10.71 Å [Figs. 3(a) and 3(b)]. The minima of energy curves in Fig. 3 should reside around 110 kcal/mol, which is slightly higher than the relative energy of CH+H in the correlation diagram in Fig. 1. Jensen function and the SM function have successful fitting results [Figs. 3(c)–3(f)]. Therefore, *ab initio* data points for very short C–H bonds are required for the SPF polynomial to behave correctly if this region is of interest.

TABLE V. The accuracy analyses of the three analytical functions. Out of the total 12 085 points, the numbers of points and corresponding ratios that are below the criterion of energy deviation.

	<±5%	<±3%	<±1%
The SPF polynomial	10 385 (86%)	9299 (77%)	7483 (62%)
Jensen function	7522 (62%)	5496 (45%)	2156 (18%)
The SM function	7919 (66%)	7108 (59%)	5239 (43%)

Selected three-dimensional graphs of the three potential energy functions are shown in Fig. 4 with either the bond angle fixed at 134.1° or one bond length fixed at 1.071 Å. Each surface is plotted using the analytical forms of corresponding fitted functions. Figures 4(a), 4(c), and 4(e) show how CH_2 dissociates into CH and H at a fixed bond distance of C–H. The surfaces are flat with various ∠HCH angles when the length of the C–H bond is 1.071 Å. With very long C–H bond, the SM function successfully reproduces this behavior [Fig. 4(e)]. Jensen function generates higher energies at small bond angles. The existence of a small exit channel barrier around 2.2 Å has been reproduced by all of the three functions. When the ∠HCH angle is fixed, the surfaces are symmetric with respect to the two C–H bonds. The surfaces are flat in the vicinity of three separate atoms, and the local minima appear around the region of CH+H [Figs. 4(b), 4(d), and 4(f)]. If ∠HCH angle is constrained at 134.1°, the surfaces of the SPF polynomial and Jensen function are correct in shape but the energy values are not constant in the dissociation region [Figs. 4(b) and 4(d)].

Our potential energy surfaces are based on *ab initio* calculations except those parameters introduced by the Morse potentials [Eqs. (9)–(11)], which are experimentally determined values. This work is a complete scanning of potential energy surface from the ground state of CH_2 to the

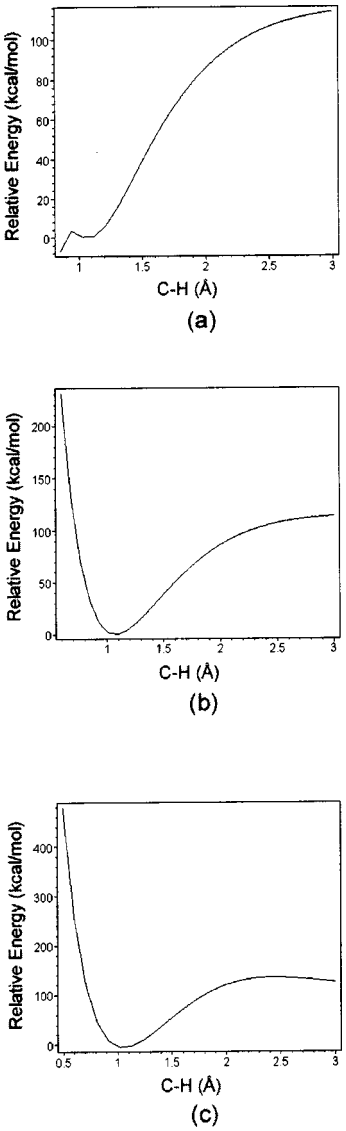

FIG. 2. The two-dimensional graph of the PES fitted by the three analytical functions with constraints of one C–H bond being 1.071 Å and ∠HCH being 134.1°: (a) the SPF polynomial, (b) Jensen function, (c) the SM function.

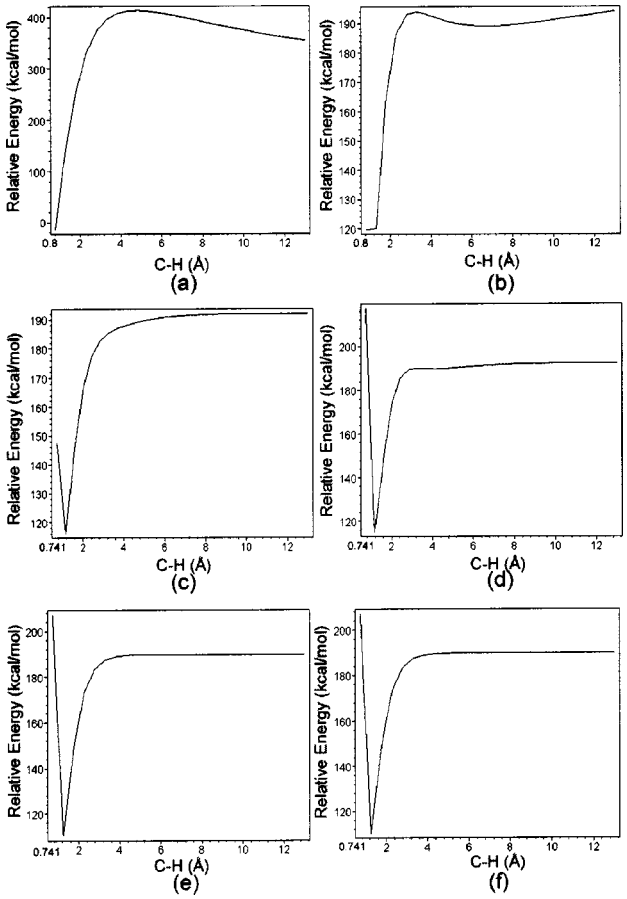

FIG. 3. The two-dimensional graph of the PES fitted by the three analytical functions with constraints of one C–H bond fixed at 10.71 Å. (a) the SPF polynomial with ∠HCH=39°, (b) the SPF polynomial with ∠HCH =134.1°, (c) Jensen function with ∠HCH=39°, (d) Jensen function with ∠HCH=134.1°, (e) the SM function with ∠HCH=39°, (f) the SM function with ∠HCH=134.1°. All energies are relative to ground state CH_2.

ground states of the three separate atoms (C+H+H). For a given geometry we can get the approximate energy and a full concept of continuity over the entire system without other considerations such as crossing. No information will be obtained about the stationary points. A contour plot of the potential energy surface with fixed ∠HCH angle of 134.1° for the ground state had been presented by Beärda *et al.* (Fig. 1 of Ref. 26) and no barrier was displayed on the surface. Their energy for dissociation into CH+H is 4.57 eV (105.39 kcal/mol), which is 1.68 kcal/mol lower than our value. Better experimental values are not available for comparison. The analytical potential function fitted by Harding *et al.*[18] is quite accurate with enough points (~6000 points) and has very low rms errors (from 0.01 kcal/mol around the equilibrium to 0.82 kcal/mol at the region of CH+H). Their potential energy surfaces are classified according to four different term symbols and details are discussed on the crossing of $^3B_1$, $^3A_2$, $^3\Pi$, and $^3\Sigma^-$ states, respectively, and are well described along these high-symmetry reaction coordinates. Their system focused on the CH_2 dissociation into CH+H and $C+H_2$, while this study also covers the dissociation region into three separate atoms.

The SPF polynomial and Jensen function are good at the description when the ∠HCH angle is fixed and close to the equilibrium value 134.1°. These two functions are proper if the regions of interest are near the equilibrium geometry of CH_2 or in the calculations of vibrational spectrums. Unsatisfactory results are obtained from the SPF polynomial and Jensen function on the course of $C+H_2$ insertion reaction because this reaction exists only when the ∠HCH angle is small. Although energy values are not perfectly accurate, the SM function will give a satisfactory description on the CH+H addition reaction. For further scattering studies, the SM function is predicted to be a better choice among the three analytical potential energy functions for that it gives a correct profile in the dissociation regions while the other two functions report too high energies at small ∠HCH angle. Thus the SM function will generate correct descriptions both in the region near the equilibrium geometry of CH_2 and the dissociation regions of CH+H as well as C+H+H.

The three-dimensional potential energy surfaces are re-

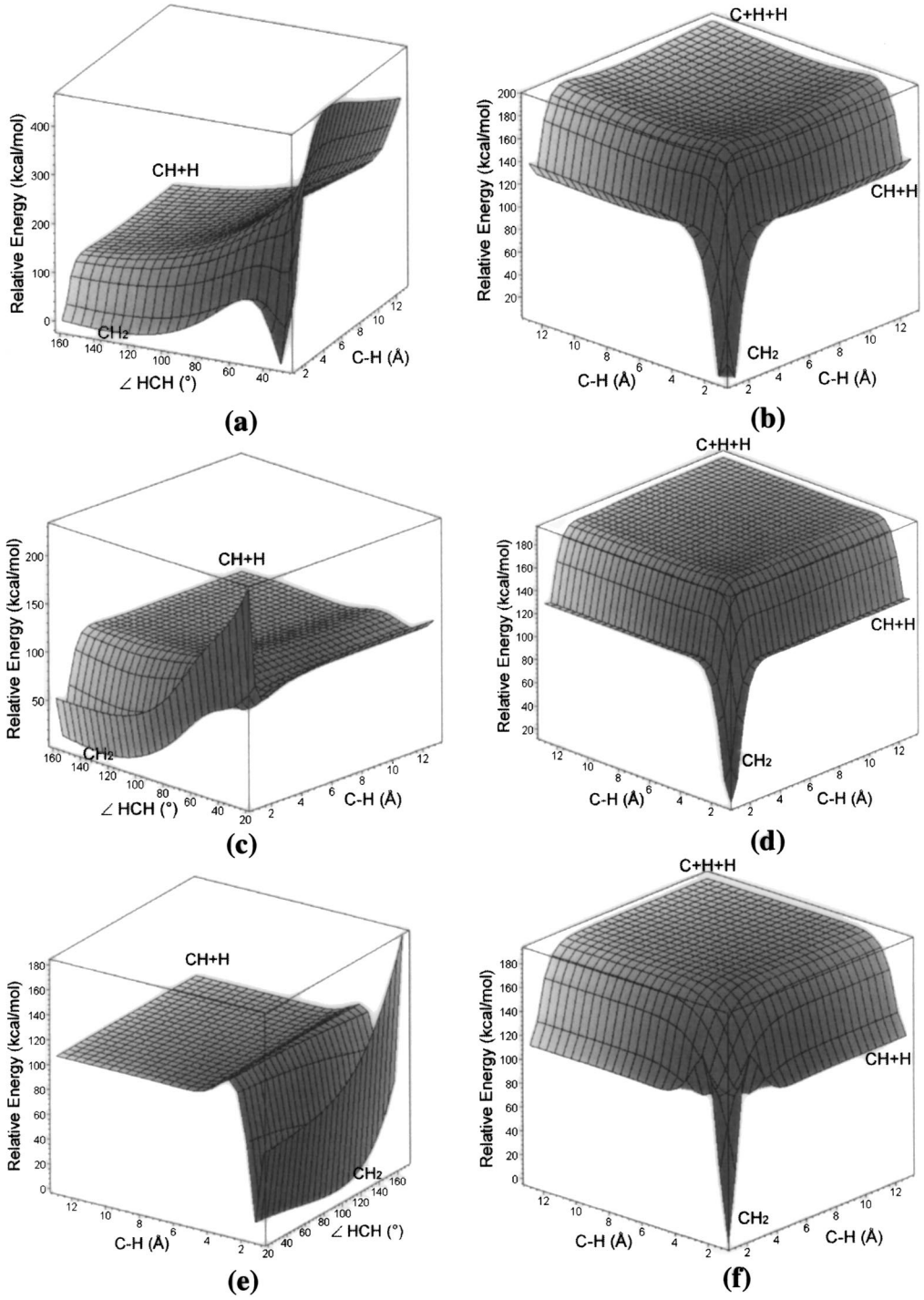

FIG. 4. The 3D graphs of fitted analytical functions: the SPF polynomial with (a) one C–H bond fixed at 1.071 Å, (b) ∠HCH fixed at 134.1°; Jensen function with (c) one C–H bond fixed at 1.071 Å, (d) ∠HCH fixed at 134.1°; as well as the SM function with (e) one C–H bond fixed at 1.071 Å, (f) ∠HCH fixed at 134.1°. All energies are relative to $CH_2(^3B_1)$.

constructed by the spline fitting on the grids in Table I. The surfaces with respect to the bond angles are shown in Fig. 5, with ∠HCH angles being 94.1°, 114.1°, 134.1°, and 174.1°. The spline fitting reproduces the exact value offered by the *ab initio* calculations, and can interpolate rather smoothly the data points that are not converged in the theoretical calculations. Even with small ∠HCH angle, the smoothness of the surface is still retained. With very large bond lengths, i.e., the frontier regions on the potential energy surfaces, the spline-fitted data points become very unreasonable as shown in Fig. 5(b). The energy rises to over 1000 kcal/mol for several points, which indicates the incapability of extrapolation by the spline fitting. It should only be applied to the regions near the equilibrium structures.

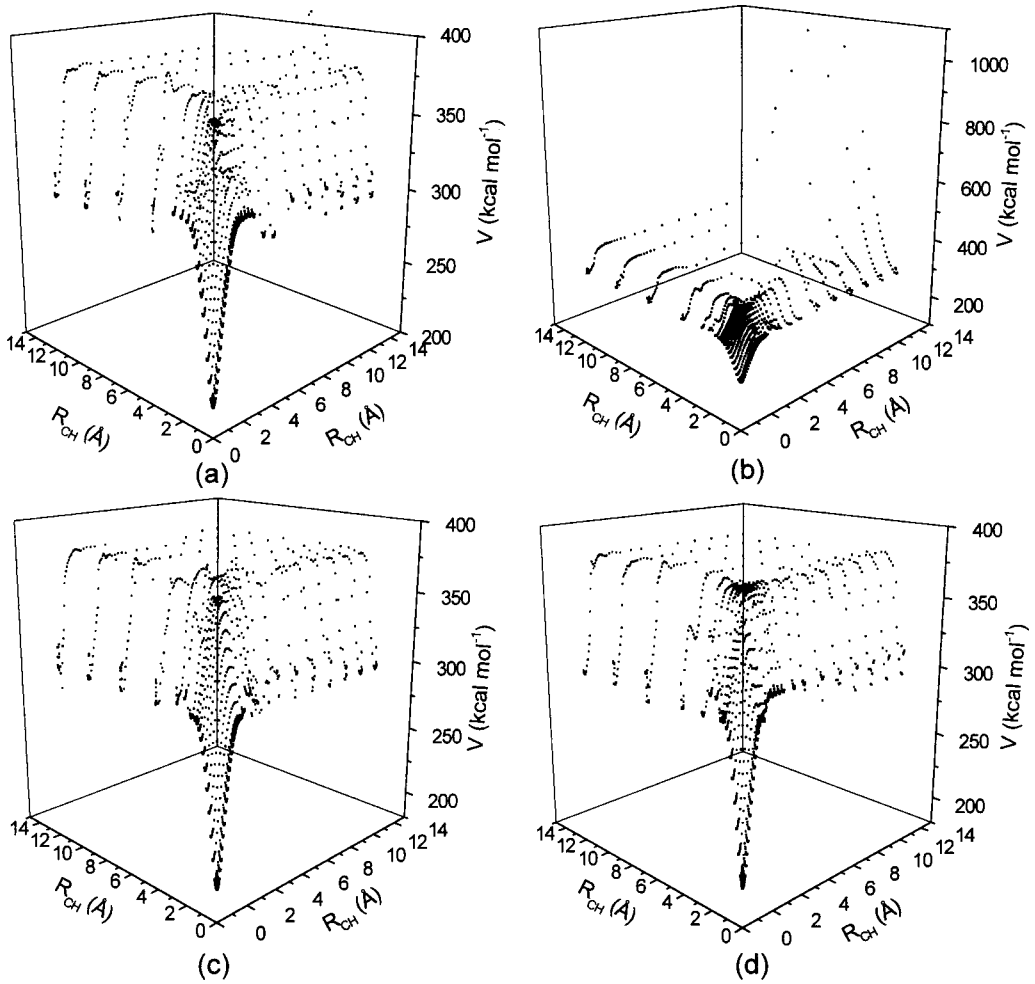

FIG. 5. The PES reconstructed by spline fitting with constraints of (a) ∠HCH=94.1°, (b) ∠HCH=114.1°, (c) HCH=134.1°, and (d) ∠HCH=174.1°.

IV. CONCLUSION

The fitting strategies do not have any consideration about symmetry factors and provides a full description of continuity over the entire region, from the ground state of CH_2 to the ground states of three separate atoms. From *ab initio* results, the bond lengths can be divided into three approximate ranges: near the equilibrium bond length, medium range, and very long distance from the equilibrium. Thus there are six combinations considering the relative energy with respect to the bond angle. Each region has its own properties. Near equilibrium, all three functions reproduce potential energy curves (relative to the minimum) upward with a local minimum as functions of bond angles with fixed bond lengths. When one of the C–H bonds is approximately at the equilibrium length and the other is slightly away from the equilibrium length, *ab initio* calculations are rather unstable. Fitting results are the poorest in this region. The variations in bond angle do not severely affect the shape of energy curves as functions of bond lengths according to *ab initio* calculations. The SM function yields invariant energy when one or both C–H bonds are sufficiently longer than the equilibrium bond length and agrees quite well with *ab initio* outputs. As shown in the 3D surface plots, the SPF produces very unreliable energetic values at very short C–H bond length. The SM function generates the features well in dissociation regions of CH+H and C+H+H. The global fit approximately produces a rms deviation of approximately 5.53 to 7.13 kcal/mol for all three potential functions. The spline fitting procedure is feasible of interpolation for the computationally divergent points within the range of *ab initio* calculations, while extrapolation can be contentious.

ACKNOWLEDGMENT

This work was supported by the National Science Council of the Republic of China under Grant No. NSC 90-2113-M-007-054.

APPENDIX: THE FUNCTIONS TO FIT THE POTENTIAL ENERGY SURFACES

For triatomic molecules, three types of empirical potential energy functions with the Born–Oppenheimer approximation are utilized, namely the Simons–Parr–Finlan polynomial, Jensen function and the Sorbie–Murrell function. The spline function featured by the algorithm of bivariate quintic polynomials is additionally employed to fit the PESs numerically.

A. The Simons–Parr–Finlan (SPF) polynomial

First introduced by G. Simons, R. G. Parr, and J. M. Finlan[27] in 1973, it was applied to diatomic molecules. Later

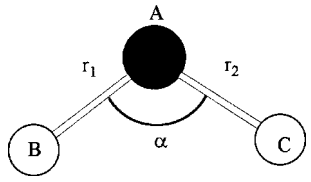

FIG. 6. The definitions of the bond lengths and bond angle in the SPF polynomial.

in 1974, G. Simons[28] slightly modified that to be employed to triatomic molecules CS_2, CO_2, etc. Having a similar form as a Taylor series, up to the quintic terms were expanded and SPF polynomial was expressed as follows with the coordinates defined in Fig. 6:

$$V=\sum_{i\leqslant j} L_{ij}\rho_i\rho_j+\sum_{i\leqslant j\leqslant k} L_{ijk}\rho_i\rho_j\rho_k+\sum_{i\leqslant j\leqslant k\leqslant l} L_{ijkl}\rho_i\rho_j\rho_k\rho_l + \sum_{i\leqslant j\leqslant k\leqslant l\leqslant m} L_{ijklm}\rho_i\rho_j\rho_k\rho_l\rho_m, \quad \text{(A1)}$$

where

$$\rho_1=\frac{r_1-r_1^e}{r_1},\quad \rho_2=\frac{r_2-r_2^e}{r_2},\quad \text{and}\quad \rho_3=\frac{\alpha-\alpha^e}{\alpha}.$$

The indices *i*, *j*, *k*, *l*, and *m* are of the numbers 1, 2, and 3. The geometric data r_1^e, r_2^e and α^e are the bond-length and bond angle values of the equilibrium geometry, and $L_{ijk}\ldots$ are the parameters required for fitting to *ab initio* values $(r_1, r_2, \alpha, W(r_1, r_2, \alpha))$. If the molecule belongs to the C_{2v} point group instead of C_s, the number of parameters would be reduced from 52 to 36. The definition of zero-energy level is the equilibrium geometry of the triatomic CH_2 molecule.

This potential function includes terms that are effectively hexic in normal coordinates displacements without introducing extra coefficients. The variables $\rho_1=(r_1-r_1^e)/r_1$ and $\rho_2=(r_2-r_2^e)/r_2$ have the correct asymmetry for a bond-stretch and behaved well as the bond lengths approach to infinity, and $\rho_3=(\alpha-\alpha^e)/\alpha$ reflects the asymmetry property of nonlinear molecules.

B. Jensen function

In 1988, P. Jensen introduced this potential function for internal-dynamics purposes.[20,21] It was expected to be sufficiently flexible for representing the PES over a wide range of triatomic molecules. In 1989, Comeau *et al.*[16] used it to get the methylene potential surface focusing on the part close to the minimum. This Jensen function has the following form where the coordinates are defined as given in Fig. 7:

$$V(\Delta r_{12}, \Delta r_{32}, \overline{\rho})=V_0(\overline{\rho})+\sum_j F_j(\overline{\rho})y_j+\sum_{j\leqslant k} F_{jk}(\overline{\rho})y_jy_k + \sum_{j\leqslant k\leqslant m} F_{jkm}(\overline{\rho})y_jy_ky_m + \sum_{j\leqslant k\leqslant m\leqslant n} F_{jkmn}(\overline{\rho})y_jy_ky_my_n, \quad \text{(A2)}$$

where Δr_{12} and Δr_{32} were two stretching coordinates that $\Delta r_{j2}=r_{j2}-r_{j2}^e$ for $j=1$ or 3, and the so-called Morse oscillator-type functions $y_j=1-\exp(-a_j\Delta r_{j2})$ for $j=1$ or 3 with a_j being molecule constants to be determined. The indices *j*, *k*, *m*, and *n* are of the values of 1 or 3. The $F_{jkm}\ldots$ expansion coefficients are functions of $\overline{\rho}$, the instaneous value of the supplement of the bond angle ρ, i.e., $\overline{\rho}=180-\rho$:[29]

$$F_j(\overline{\rho})=\sum_{i=1}^{4} f_j^{(i)}(\cos\rho_e-\cos\overline{\rho})^i, \quad \text{(A3)}$$

$$F_{jk}(\overline{\rho})=f_{jk}^{(0)}+\sum_{i=1}^{3} f_{jk}^{(i)}(\cos\rho_e-\cos\overline{\rho})^i, \quad \text{(A4)}$$

$$F_{jkm}(\overline{\rho})=f_{jkm}^{(0)}+\sum_{i=1}^{2} f_{jkm}^{(i)}(\cos\rho_e-\cos\overline{\rho})^i, \quad \text{(A5)}$$

$$F_{jkmn}(\overline{\rho})=f_{jkmn}^{(0)}+f_{jkmn}^{(1)}(\cos\rho_e-\cos\overline{\rho}). \quad \text{(A6)}$$

ρ_e is the equilibrium of $\overline{\rho}$. Those $f_{jkm}\ldots$ are the parameters which to be optimized by fitted to *ab initio* values during the surface fitting process.

The pure bending potential energy function, the one for the molecular bending with the bond lengths fixed at their equilibrium values and denoted as $V_0(\overline{\rho})$, is parametrized as

$$V_0(\overline{\rho})=\sum_{i=1}^{8} f_0^{(i)}(\cos\rho_e-\cos\overline{\rho})^i. \quad \text{(A7)}$$

Similarly, $f_0^{(i)}\ldots$ are the parameters.

The expression for this potential function, which constitutes rapidly converging power series, is to have a physically reasonable asymptotic behavior at all coordinate boundaries. For $\overline{\rho}=0$ and 180 with any values of r_{12} and r_{32}, the first derivative of the potential function is zero. For large values of r_{12} and r_{32}, it approaches to a constant for any value of $\overline{\rho}$, and for small r_{12} and r_{32}, it approaches to a very large value, but not infinite.

The total number of parameters is 51. For a molecule of C_{2v} point group, a_1 equals to a_3, and symmetry relations exists between the parameters so that *V* is totally symmetric under the exchange of y_1 and y_3. Thus the number of parameters is reduced to 36. In addition, the zero of the potential energy is set to where the triatomic molecule resides at its equilibrium geometry.

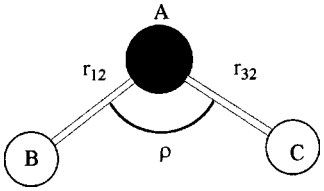

FIG. 7. The definitions of the bond lengths and bond angle in Jensen function.

C. The Sorbie–Murrell (SM) function

K. S. Sorbie and J. N. Murrell constructed this analytical function[30] in 1975 for the ground states of stable triatomic

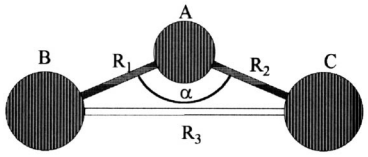

FIG. 8. The definitions of the bond lengths and bond angle in the SM function.

molecules from spectroscopic data, aiming to reproduce both the equilibrium and asymptotic properties of the molecule. It was first applied to water molecule. Later, this potential function was used for CH_2,[31] $H+CO$,[32–34] and HCO.[35,36]

This SM function $V(R_1,R_2,R_3)$ is only applicable for molecules which have nonlinear equilibrium geometry. Three out of the four terms of the SM function are for diatomic potentials and the other term is a three-body term. The mathematical expression is as follows shown in Fig. 8:

$$V(R_1,R_2,R_3)=V_{AB}(R_1)+V_{AC}(R_2)+V_{BC}(R_3)+V_I(R_1,R_2,R_3), \tag{A8}$$

$$V_{AB}(R_1)=De_1\{-2\exp[-\beta e_1(R_1-R_{AB})]+\exp[-2\beta e_1(R_1-R_{AB})]\}, \tag{A9}$$

$$V_{AC}(R_2)=De_2\{-2\exp[-\beta e_2(R_2-R_{AC})]+\exp[-2\beta e_2(R_2-R_{AC})]\}, \tag{A10}$$

$$V_{BC}(R_3)=De_3\{-2\exp[-\beta e_3(R_3-R_{BC})]+\exp[-2\beta e_3(R_3-R_{BC})]\}. \tag{A11}$$

The terms V_{AB}, V_{AC}, and V_{BC} are Morse potentials, where R_{AB}, R_{AC}, and R_{BC} are the diatomic equilibrium bond lengths of AB, AC, and BC, respectively. The zero-energy level of the Morse potentials are set at where two atoms are in their individual ground states.

The three-body term V_I has the following form:

$$V_I(R_1,R_2,R_3)=AP(s_1,s_2,s_3)[1-\tanh(\gamma_1 s_1/2)]\times[1-\tanh(\gamma_2 s_2/2)][1-\tanh(\gamma_3 s_3/2)], \tag{A12}$$

where s_1, s_2, s_3 defined as $s_i=R_i-R_{ie}$ with $i=1$, 2, and 3 being displacements from the triatomic equilibrium distances, R_{1e}, R_{2e}, and R_{3e} and A, γ_1, γ_2, and γ_3, are parameters.

$P(s_1,s_2,s_3)$ in Eq. (A12) is a polynomial up to the cubic terms

$$\begin{aligned}P(s_1,s_2,s_3)=&c_0+c_1s_1+c_2s_2+c_3s_3\,(c_{11}s_1^2+c_{22}s_2^2+c_{33}s_3^2)\\&+c_{12}s_1s_2+c_{13}s_1s_3+c_{23}s_2s_3+\tfrac{1}{6}(c_{111}s_1^3\\&+c_{222}s_2^3+c_{333}s_3^3)+\tfrac{1}{2}(c_{112}s_1^2s_2+c_{113}s_1^2s_3\\&+c_{122}s_1s_2^2+c_{133}s_1s_3^2+c_{223}s_2^2s_3+c_{233}s_2s_3^2)\\&+c_{123}s_1s_2s_3,\end{aligned} \tag{A13}$$

where c_0 is a parameter and c_i, c_{ij}, and c_{ijk} are constants and to be derived later.

The zero of energy of this SM function is the ground state of three separate atoms. The condition is imposed that V_I becomes zero at all dissociation limits and this is controlled by $[1-\tanh(\gamma_1 s_1/2)][1-\tanh(\gamma_2 s_2/2)][1-\tanh(\gamma_3 s_3/2)]$. The term $[1-\tanh(\gamma_i s_i/2)]$ has the property of being zero as s_i approaches to positive infinity and being a constant of 2 as s_i gets close to negative infinity. The Morse potentials are then the potentials of appropriate electronic states of the diatomic dissociation products.

There is no cusp on the potential energy surface in this study. In order to get the values of coefficients in $P(s_1,s_2,s_3)$, the first step is to use the *ab initio* values to get the derivatives and force constants in the Talor polynomial. With internal coordinates (R_1,R_2,α) being used and up to the cubic terms being expanded, the Talor polynomial is

$$\begin{aligned}W(R_1,R_2,\alpha)=&W(R_{1e},R_{2e},\alpha_e)+\tfrac{1}{2}[f_{11}(R_1-R_{1e})^2+f_{22}(R_2-R_{2e})^2f_{\alpha\alpha}(\alpha-\alpha_e)^2]+f_{12}(R_1-R_{1e})(R_2-R_{2e})\\&+f_{1\alpha}(R_1-R_{1e})(\alpha-\alpha_e)+f_{2\alpha}(R_2-R_{2e})(\alpha-\alpha_e)+\tfrac{1}{6}[f_{111}(R_1-R_{1e})^3+f_{222}(R_2-R_{2e})^3\\&+f_{\alpha\alpha\alpha}(\alpha_3-\alpha_e)^3]+\tfrac{1}{2}[f_{112}(R_1-R_{1e})^2(R_2-R_{2e})+f_{122}(R_1-R_{1e})(R_2-R_{2e})^2+f_{11\alpha}(R_1-R_{1e})^2(\alpha-\alpha_e)\\&+f_{1\alpha\alpha}(R_1-R_{1e})(\alpha-\alpha_e)^2+f_{22\alpha}(R_2-R_{2e})^2(\alpha-\alpha_e)+f_{2\alpha\alpha}(R_2-R_{2e})(\alpha-\alpha_e)^2]\\&+f_{12\alpha}(R_1-R_{1e})(R_2-R_{2e})(\alpha-\alpha_e).\end{aligned} \tag{A14}$$

The first-order derivatives are not appeared above because at the equilibrium geometry, the potential is a minimum and thus those terms are all zero.

The force constants that are represented in the coordinate set (R_1, R_2, α) must be converted to those in the set (R_1, R_2, R_3). The relevant transformations start from the derivatives of α with respect to R_1, R_2, and R_3, which are related by the law of cosine,

$$\alpha=a\cos\left(\frac{R_1^2+R_2^2-R_3^2}{2R_1R_2}\right), \tag{A15}$$

$$Z=-R_{1e}^4+2R_{1e}^2(R_{2e}^2+R_{3e}^2)-R_{2e}^4+R_{3e}^2(2R_{2e}^2-R_{3e}^2). \tag{A16}$$

The following listed all the expressions of the derivatives $\alpha_{ijk}\ldots$ calculated at the equilibrium geometry (R_{1e}, R_{2e}, R_{3e}):

$$\alpha_1=\frac{-R_{1e}^2+R_{2e}^2-R_{3e}^2}{R_{1e}\sqrt{Z}}, \tag{A17}$$

$$\alpha_2=\frac{R_{1e}^2-R_{2e}^2-R_{3e}^2}{R_{2e}\sqrt{Z}}, \tag{A18}$$

$$\alpha_3=\frac{2R_{3e}}{\sqrt{Z}}, \tag{A19}$$

$$\begin{aligned}\alpha_{11}=&-\frac{1}{2R_{1e}^2Z\sqrt{Z}}[R_{1e}^6+3R_{1e}^4(R_{3e}^2-R_{2e}^2)\\&+R_{1e}^2(3R_{2e}^4+2R_{2e}^2R_{3e}^2-5R_{3e}^4)\\&+(R_{3e}^2-R_{2e}^2)(R_{2e}^4-2R_{2e}^2R_{3e}^2+R_{3e}^4)],\end{aligned} \tag{A20}$$

$$\begin{aligned}\alpha_{22}=&\frac{1}{R_{2e}^2Z\sqrt{Z}}[R_{1e}^6-3R_{1e}^4(R_{3e}^2+R_{2e}^2)\\&+R_{1e}^2(3R_{2e}^4-2R_{2e}^2R_{3e}^2+3R_{3e}^4)\\&+(R_{3e}^2-R_{2e}^2)(R_{2e}^4+4R_{2e}^2R_{3e}^2-R_{3e}^4)],\end{aligned} \tag{A21}$$

$$\alpha_{33}=\frac{2}{\sqrt{Z}}-\frac{4R_{3e}^2(R_{1e}^2+R_{2e}^2-R_{3e}^2)}{Z\sqrt{Z}}, \tag{A22}$$

$$\alpha_{12}=\frac{8R_{1e}R_{2e}R_{3e}^2}{Z\sqrt{Z}}, \tag{A23}$$

$$\alpha_{13}=\frac{4R_{1e}R_{3e}(R_{1e}^2-R_{2e}^2-R_{3e}^2)}{Z\sqrt{Z}}, \tag{A24}$$

$$\alpha_{23}=\frac{4R_{2e}R_{3e}(R_{2e}^2-R_{1e}^2-R_{3e}^2)}{Z\sqrt{Z}}, \tag{A25}$$

$$\begin{aligned}\alpha_{111}=&\frac{2(R_{2e}^2-R_{3e}^2)}{R_{1e}^3\sqrt{Z}}\\&-\frac{2[5R_{1e}^4-2R_{1e}^2(2R_{2e}^2+R_{3e}^2)+R_{3e}^4-2R_{2e}^2]}{R_{1e}Z\sqrt{Z}}\\&-\frac{12R_{1e}(R_{1e}^2-R_{2e}^2+R_{3e}^2)(R_{1e}^2-R_{2e}^2-R_{3e}^2)^2}{Z^2\sqrt{Z}},\end{aligned} \tag{A26}$$

$$\begin{aligned}\alpha_{222}=&\frac{2(R_{1e}^2-R_{3e}^2)}{R_{2e}^3\sqrt{Z}}\\&+\frac{2[R_{1e}^4+4R_{1e}^2R_{2e}^2-5R_{2e}^4+2R_{2e}^2R_{3e}^2-R_{3e}^4]}{R_{2e}Z\sqrt{Z}}\\&-\frac{12R_{2e}(R_{1e}^2-R_{2e}^2-R_{3e}^2)(R_{1e}^2-R_{2e}^2+R_{3e}^2)^2}{Z^2\sqrt{Z}},\end{aligned} \tag{A27}$$

$$\begin{aligned}\alpha_{333}=&\frac{4R_{3e}}{Z^2\sqrt{Z}}[3R_{1e}^6-R_{1e}^4(3R_{2e}^2+5R_{3e}^2)\\&-R_{1e}^2(3R_{2e}^4-10R_{2e}^2R_{3e}^2-3R_{3e}^4)\\&+(3R_{2e}^2+R_{3e}^2)(R_{2e}^4-2R_{2e}^2R_{3e}^2+3R_{3e}^4)],\end{aligned} \tag{A28}$$

$$\alpha_{112}=\frac{8R_{2e}R_{3e}^2[5R_{1e}^4-4R_{1e}^2(R_{2e}^2+R_{3e}^2)-R_{2e}^4+2R_{2e}^2R_{3e}^2-R_{3e}^4]}{Z^2\sqrt{Z}}, \tag{A29}$$

$$\alpha_{122}=-\frac{8R_{1e}R_{3e}^2[R_{1e}^4+2R_{1e}^2(2R_{2e}^2-R_{3e}^2)-5R_{2e}^4+R_{3e}^2(4R_{2e}^2+R_{3e}^2)]}{Z^2\sqrt{Z}}, \tag{A30}$$

$$\begin{aligned}\alpha_{113}=&\frac{2R_{3e}}{R_{1e}^2\sqrt{Z}}+\frac{2R_{3e}[R_{1e}^4+2R_{1e}^2(R_{2e}^2+R_{3e}^2)+R_{2e}^4-2R_{2e}^2R_{3e}^2+R_{3e}^4]}{R_{1e}^2Z\sqrt{Z}}\\&+\frac{12R_{3e}(R_{1e}^2-R_{2e}^2-R_{3e}^2)(R_{1e}^2+R_{2e}^2-R_{3e}^2)(R_{1e}^2-R_{2e}^2+R_{3e}^2)}{Z^2\sqrt{Z}},\end{aligned} \tag{A31}$$

$$\alpha_{133}=-\frac{4R_{1e}}{Z^2\sqrt{Z}}[R_{1e}^6+R_{1e}^4(R_{3e}^2-3R_{2e}^2)+R_{1e}^2(3R_{2e}^4+6R_{2e}^2R_{3e}^2-5R_{3e}^4)-R_{2e}^6-R_{3e}^2(7R_{2e}^4-5R_{2e}^2R_{3e}^2-3R_{3e}^4), \tag{A32}$$

$$\begin{aligned}\alpha_{223}=&\frac{2R_{3e}}{R_{2e}^2\sqrt{Z}}+\frac{2R_{3e}[R_{1e}^4+2R_{1e}^2(R_{2e}^2-R_{3e}^2)+R_{2e}^4+2R_{2e}^2R_{3e}^2+R_{3e}^4]}{R_{2e}^2Z\sqrt{Z}}\\&+\frac{12R_{3e}(R_{1e}^2-R_{2e}^2-R_{3e}^2)(R_{1e}^2+R_{2e}^2-R_{3e}^2)(R_{1e}^2-R_{2e}^2+R_{3e}^2)}{Z^2\sqrt{Z}},\end{aligned} \tag{A33}$$

$$\alpha_{233}=-\frac{4R_{2e}}{Z^2\sqrt{Z}}[R_{1e}^6+R_{1e}^4(7R_{3e}^2-3R_{2e}^2)+R_{1e}^2(3R_{2e}^4-6R_{2e}^2R_{3e}^2-5R_{3e}^4)-R_{2e}^6+R_{3e}^2(-R_{2e}^4+5R_{2e}^2R_{3e}^2-3R_{3e}^4), \tag{A34}$$

$$\alpha_{123}=-\frac{16R_{1e}R_{2e}R_{3e}[R_{1e}^4+R_{1e}^2(2R_{2e}^2-R_{3e}^2)+R_{2e}^4+R_{2e}^2R_{3e}^2-2R_{3e}^4]}{Z^2\sqrt{Z}}. \tag{A35}$$

The formula of force constants in $V(R_1,R_2,R_3)$ are in terms of $\alpha_{ijk}\ldots$ and $f_{ijk}\ldots$. The exact forms are not shown here; they are accompanied to appear instead in the expressions for the force constants in $V_I(R_1,R_2,R_3)$.

By making a Talor series of the right-hand side of the equation listed below, Eq. (A36), there is a one-to-one correspondence between the derivatives and the coefficients of $P(s_1,s_2,s_3)$.

$$P(s_1,s_2,s_3)=AV_I(R_1,R_2,R_3)[1-\tanh(\gamma_1 s_1/2)]^{-1}\times[1-\tanh(\gamma_2 s_2/2)]^{-1}[1-\tanh(\gamma_3 s_3/2)]^{-1}. \tag{A36}$$

The force constants in the Taylor series of V_I around the equilibrium geometry are not directly obtained, but are derived from the equality $V_I=V-V_{AB}-V_{AC}-V_{BC}$. Since the force constants in V are known and it is not difficult to get those force constants in Morse potentials:

$$g_1=\frac{\gamma_1}{2}, \tag{A37}$$

$$g_2=\frac{\gamma_2}{2}, \tag{A38}$$

$$g_3=\frac{\gamma_3}{2}, \tag{A39}$$

$$G_{ij}=\frac{1}{A}\left(\frac{\partial^2 V_I}{\partial s_i\partial s_j}\right)_{s_i=0,s_j=0},$$

$$G_{11}=\frac{1}{A}(f_{11}+2\alpha_1 f_{1\alpha}+\alpha_1^2 f_{\alpha\alpha}-2\beta e_1^2 D_{e1}), \tag{A40}$$

$$G_{22}=\frac{1}{A}(f_{22}+2\alpha_2 f_{2\alpha}+\alpha_2^2 f_{\alpha\alpha}-2\beta e_2^2 D_{e2}), \tag{A41}$$

$$G_{33}=\frac{1}{A}(\alpha_3^2 f_{\alpha\alpha}-2\beta e_3^2 D_{e3}), \tag{A42}$$

$$G_{12}=\frac{1}{A}(f_{12}+\alpha_2 f_{1\alpha}+\alpha_1 f_{2\alpha}+\alpha_1\alpha_2 f_{\alpha\alpha}), \tag{A43}$$

$$G_{13}=\frac{1}{A}(\alpha_3 f_{1\alpha}+\alpha_1\alpha_3 f_{\alpha\alpha}), \tag{A44}$$

$$G_{23}=\frac{1}{A}(\alpha_3 f_{2\alpha}+\alpha_2\alpha_3 f_{\alpha\alpha}), \tag{A45}$$

$$G_{111}=\frac{1}{A}[f_{111}+3\alpha_1(f_{11\alpha}+\alpha_1 f_{1\alpha\alpha})+\alpha_1^3 f_{\alpha\alpha\alpha}+3\alpha_{11}(f_{1\alpha}+\alpha_1 f_{\alpha\alpha})+6\beta e_1^3 D_{e1}], \tag{A46}$$

$$G_{222}=\frac{1}{A}[f_{222}+3\alpha_2(f_{22\alpha}+\alpha_2 f_{2\alpha\alpha})+\alpha_2^3 f_{\alpha\alpha\alpha}+3\alpha_{22}(f_{2\alpha}+\alpha_2 f_{\alpha\alpha})+6\beta e_2^3 D_{e2}], \tag{A47}$$

$$G_{333}=\frac{1}{A}[\alpha_3(\alpha_3^2 f_{\alpha\alpha\alpha}+3\alpha_{33}f_{\alpha\alpha})+6\beta e_2^3 D_{e2}], \tag{A48}$$

$$G_{112}=\frac{1}{A}[f_{112}+\alpha_2 f_{11\alpha}+2\alpha_1(f_{12\alpha}+\alpha_2 f_{1\alpha\alpha})+\alpha_1^2(f_{2\alpha\alpha}+\alpha_2 f_{\alpha\alpha\alpha})+2\alpha_{12}f_{1\alpha}+\alpha_{11}f_{2\alpha}+f_{\alpha\alpha}(2\alpha_1\alpha_{12}+\alpha_2\alpha_{11})], \tag{A49}$$

$$G_{113}=\frac{1}{A}[\alpha_3(f_{11\alpha}+2\alpha_1 f_{1\alpha\alpha}+\alpha_1^2 f_{\alpha\alpha\alpha})+2\alpha_{13}f_{1\alpha}+f_{\alpha\alpha}(2\alpha_1\alpha_{13}+\alpha_3\alpha_{11})], \tag{A50}$$

$$G_{122}=\frac{1}{A}[f_{122}+\alpha_1 f_{22\alpha}+2\alpha_2(f_{12\alpha}+\alpha_1 f_{2\alpha\alpha})+\alpha_2^2(f_{1\alpha\alpha}+\alpha_1 f_{\alpha\alpha\alpha})], \tag{A51}$$

$$G_{133}=\frac{1}{A}[\alpha_3^2(f_{1\alpha\alpha}+\alpha_1 f_{\alpha\alpha\alpha})+\alpha_{33}f_{1\alpha}+f_{\alpha\alpha}(2\alpha_3\alpha_{13}+\alpha_1\alpha_{33})], \tag{A52}$$

$$G_{223}=\frac{1}{A}[\alpha_3(f_{22\alpha}+2\alpha_2 f_{2\alpha\alpha}+\alpha_2^2 f_{\alpha\alpha\alpha})+2\alpha_{23}f_{2\alpha}+f_{\alpha\alpha}(2\alpha_2\alpha_{23}+\alpha_3\alpha_{22})], \tag{A53}$$

$$G_{233}=\frac{1}{A}[\alpha_3^2(f_{2\alpha\alpha}+\alpha_2 f_{\alpha\alpha\alpha})+\alpha_{33}f_{2\alpha}+f_{\alpha\alpha}(2\alpha_3\alpha_{23}+\alpha_2\alpha_{33})], \tag{A54}$$

$$G_{123}=\frac{1}{A}[\alpha_3(f_{12\alpha}+\alpha_2 f_{1\alpha\alpha}+\alpha_1 f_{2\alpha\alpha}+\alpha_1\alpha_2 f_{\alpha\alpha\alpha})+\alpha_{23}f_{1\alpha}+\alpha_{13}f_{2\alpha}+f_{\alpha\alpha}(\alpha_1\alpha_{23}+\alpha_2\alpha_{13}+\alpha_3\alpha_{12})]. \tag{A55}$$

In the above formula, only in G_{11}, G_{22}, G_{33}, G_{111}, G_{222}, and G_{333} appear in the βe and D_e terms. They are contributed from Morse potentials. Finally the coefficients in $P(s_1,s_2,s_3)$ can be expressed in terms of g_i, G_{ij}, etc.:

$$c_1 = g_1, \tag{A56}$$

$$c_2 = g_2, \tag{A57}$$

$$c_3 = g_3, \tag{A58}$$

$$c_{11} = g_1^2 + \tfrac{1}{2} G_{11}, \tag{A59}$$

$$c_{22} = g_2^2 + \tfrac{1}{2} 12\, G_{22}, \tag{A60}$$

$$c_{33} = g_3^2 + \tfrac{1}{2} G_{33}, \tag{A61}$$

$$c_{12} = g_1 g_2 + G_{12}, \tag{A62}$$

$$c_{13} = g_1 g_3 + G_{13}, \tag{A63}$$

$$c_{23} = g_2 g_3 + G_{23}, \tag{A64}$$

$$c_{111} = \tfrac{2}{3} g_1^3 + \tfrac{1}{2} g_1 G_{11} + \tfrac{1}{6} G_{111}, \tag{A65}$$

$$c_{222} = \tfrac{2}{3} g_2^3 + \tfrac{1}{2} g_2 G_{22} + \tfrac{1}{6} G_{222}, \tag{A66}$$

$$c_{333} = \tfrac{2}{3} g_3^3 + \tfrac{1}{2} g_3 G_{33} + \tfrac{1}{6} G_{333}, \tag{A67}$$

$$c_{112} = g_1^2 g_2 + g_1 G_{12} + \tfrac{1}{2} g_2 G_{11} + \tfrac{1}{2} G_{112}, \tag{A68}$$

$$c_{113} = g_1^2 g_3 + g_1 G_{13} + \tfrac{1}{2} g_3 G_{11} + \tfrac{1}{2} G_{113}, \tag{A69}$$

$$c_{122} = g_1 g_2^2 + g_2 G_{12} + \tfrac{1}{2} g_1 G_{22} + \tfrac{1}{2} G_{122}, \tag{A70}$$

$$c_{133} = g_1 g_3^2 + g_3 G_{13} + \tfrac{1}{2} g_1 G_{33} + \tfrac{1}{2} G_{133}, \tag{A71}$$

$$c_{223} = g_3^2 g_3 + g_2 G_{13} + \tfrac{1}{2} g_3 G_{22} + \tfrac{1}{2} G_{223}, \tag{A72}$$

$$c_{233} = g_2 g_3^2 + g_3 G_{23} + \tfrac{1}{2} g_2 G_{33} + \tfrac{1}{2} G_{233}, \tag{A73}$$

$$c_{123} = g_1 g_2 g_3 + g_1 G_{23} + g_2 G_{13} + g_3 G_{12} + G_{123}. \tag{A74}$$

After substituting the coefficients into the polynomial, the analytical potential function is completed and the five parameters (γ_1, γ_2, γ_3, c_0, A) are to be optimized.

D. The bivariate spline fitting

The bivariate spline fitting aims to calculate a C^1 interpolant to scattered data in a plane. For the data points $\{(x_i, y_i, V_i)\}_{i=1}^N$ in R^3, the interpolant s is computed by firstly the Delaunay triangulation of the points $\{(x_i, y_i)\}_{i=1}^N$. In this triangulation on each triangular T, the s has the form

$$s(x, y) = \sum_{m+n \leqslant 5} c_{mn}^T x^m y^n \ \forall x, y \in T. \tag{A75}$$

Therefore on each triangle of this triangulation, s is a bivariate quintic polynomial. Additionally, $s(x_i, y_i) = V_i$ for $i = 1, 2, \ldots, N$, and s is continuously differentiable across the boundaries of nearby triangles.

The output points by our *ab initio* results are grouped into separate data sets of identical bond angles. Each data set with the fixed constant bond angle is then fitted using the preceding bivariate quintic polynomial with x_i and y_i being the two bond lengths.

[1] P. W. Atkins, Physical Chemistry (Oxford University Press, Oxford, 1990), pp. 862–867.
[2] D. G. Truhlar, F. B. Brown, D. W. Schwenke, R. Steckler, and B. C. Garrett, in *Comparison of Ab Initio Quantum Chemistry with Experiment for Small Molecules*, edited by R. J. Barlett (Reidel, Holland, 1985), pp. 95–140.
[3] P. R. Bunker, in *Comparison of Ab Initio Quantum Chemistry with Experiment for Small Molecules*, edited by R. J. Barlett (Reidel, Holland, 1985), pp. 141–170.
[4] W. Reuter, B. Engels, and S. D. Peyerimhoff, J. Phys. Chem. **96**, 6221 (1992), and references therein.
[5] J. March, *Advanced Organic Chemistry*, 2nd ed. (McGraw-Hill, New York, 1977).
[6] I.-C. Chen, W. H. Green, Jr., and C. B. Moore, J. Chem. Phys. **89**, 314 (1988).
[7] J. F. Liebman and J. Simons, *Molecular Structure and Energetics*, Vol. V, edited by J. F. Liebman and A. Greenberg (VCH, Florida, 1986), Chap. 3.
[8] R. B. Beärda, M. C. vanHemert, and E. F. van Dishoeck, J. Chem. Phys. **97**, 8240 (1992).
[9] G. J. Kroes, E. F. van Dishoeck, R. B. Beärda, and M. C. vanHemert, J. Chem. Phys. **99**, 228 (1993).
[10] R. J. Blint, and M. D. Newton, Chem. Phys. Lett. **32**, 178 (1975).
[11] M. E. Casida, M. M. L. Chen, R. D. MacGregor, and H. F. Schaefer III, Isr. J. Chem. **19**, 127 (1980).
[12] P. Knowles, N. C. Handy, and S. Carter, Mol. Phys. **49**, 681 (1983).
[13] L. B. Harding, J. Phys. Chem. **87**, 441 (1983).
[14] A. D. McLean, P. R. Bunker, R. M. Escribano, and P. Jensen, J. Chem. Phys. **87**, 2166 (1987).
[15] P. Jensen and P. R. Bunker, J. Chem. Phys. **89**, 1327 (1988).
[16] D. C. Comeau, I. Shavitt, P. Jensen, and P. R. Bunker, J. Chem. Phys. **90**, 6491 (1989).
[17] R. A. Beärda, M. C. vanHemert, and E. F. Van Dishoeck, J. Chem. Phys. **97**, 8240 (1992).
[18] L. B. Harding, R. Guadagnini, and G. C. Schatz, J. Phys. Chem. **97**, 5472 (1993).
[19] V. J. Barclay, I. P. Hamilton, and P. Jensen, J. Chem. Phys. **99**, 9709 (1993).
[20] P. Jensen, J. Mol. Spectrosc. **128**, 478 (1988).
[21] P. Jensen, J. Chem. Soc., Faraday Trans. 2 **84**, 1315 (1988).
[22] J. P. Watts, J. Gauss, and R. J. Barlett, J. Chem. Phys. **98**, 8718 (1993).
[23] ACES II is a program product of the Quantum Theory Project, University of Florida. Authors: J. F. Stanton, J. Gauss, J. D. Watts *et al.* Integral packages included are VMOL (J. Almlöf and P. R. Taylor); VPROPS (P. Taylor) ABACUS (T. Helgaker, H. J. Aa. Jensen, P. Jørgensen, J. Olsen, and P. R. Taylor).
[24] J. E. Dennis, Jr. and R. B. Schnabel, *Numerical Methods for Unconstrained Optimization and Nonlinear Equations* (Prentice-Hall, New Jersey, 1983); K. Levenberg, Q. Appl. Math. **2**, 164 (1944); D. Marquardt, SIAM (Soc. Ind. Appl. Math.) J. Appl. Math. **11**, 431 (1963); Moré, Jorge, B. Garbow, and K. Hillstorm, *User Guide for MINPACK-1*, Argonne National Labs Report ANL-80-74, Argonne, Illinois (1980).
[25] M. D. Marshall and A. R. W. McKellar, J. Chem. Phys. **85**, 3716 (1986).
[26] R. A. Beärda, G.-J. Kroes, M. C. Hemert, B. Heumann, R. Schinke, and E. F. vanDishoeck, J. Chem. Phys. **100**, 1113 (1994).
[27] G. Simons, R. G. Parr, and J. M. Finlan, J. Chem. Phys. **59**, 3229 (1973).
[28] G. Simons, J. Chem. Phys. **61**, 369 (1974).
[29] J. T. Hougen, P. R. Bunker, and J. W. C. Johns, J. Mol. Spectrosc. **34**, 136 (1970).
[30] K. S. Sorbie and J. N. Murrell, Mol. Phys. **29**, 1387 (1975).
[31] M. J. Redmon and G. C. Schatz, Chem. Phys. **54**, 365 (1981).
[32] S. Carter, I. M. Mills, and J. N. Murrell, J. Chem. Soc., Faraday Trans. 2 **1**, 148 (1979).
[33] G. C. Schatz and H. Elgersma, Chem. Phys. Lett. **73**, 21 (1980).
[34] L. C. Geiger and G. C. Schatz, J. Phys. Chem. **88**, 214 (1984).
[35] G. Kroes, E. F. van Dishoeck, R. A. Beärda, and M. C. vanHemert, J. Chem. Phys. **99**, 228 (1993).
[36] P. R. Bunker and P. Jensen, J. Chem. Phys. **79**, 1224 (1983).